

Polyampholyte-Dressed Micelles of Fluorinated and Hydrogenated Dodecanoic Acid

Andreas F. Thünemann,* Kathrin Sander, and Werner Jaeger

Fraunhofer Institute for Applied Polymer Research, Geiselbergstrasse 69,
D-14476 Golm, Germany

Rumiana Dimova

Max Planck Institute of Colloid and Interfaces, Am Mühlenberg 2, D-14476 Golm, Germany

Received February 20, 2002. In Final Form: April 15, 2002

Polyampholytes with alternating cationic and anionic monomers were synthesized and complexed with fatty acids (dodecanoic acid and perfluorododecanoic acid). The formation of the polyelectrolyte–fatty acid complexes is self-assembled and generates nanoparticles with sizes in the range of 3–5 nm that were named dressed micelles. A defined arrangement of the ionic charges of three polyampholytes was achieved by the copolymerization of a cationic vinyl monomer (*N,N*-diallyl-*N,N*-dimethylammonium chloride) and anionic vinyl monomers (maleamic acid, phenylmaleamic acid, and 4-butylphenylmaleamic acid). The zeta potentials of the polyampholyte dressed micelles were adjusted in the range of –56 to 25 mV. They increase when replacing the alkylated dodecanoic acid by its perfluorinated counterpart, and they also increase when enhancing the hydrophilicity of the polyampholyte. Analytical ultracentrifugation, dynamic light scattering, and isothermal titration calorimetry were used for the characterization of the fluorinated and the hydrogenated complexes.

Introduction

The complexation of polyelectrolytes with low molecular weight amphiphiles (ionic surfactants, fatty acids) produces self-assembled soft matter that combines the properties of polymers such as mechanical stability with the capability of surfactants to form supramolecular ordered structures, for example, smectic and hexagonal phases. Reviews of this field are given by Thou and Chu,¹ by Ober and Wegner,² and also by Tirrell et al.³ The interaction of polymers and surfactants results typically in the formation of water-insoluble complexes⁴ if the stoichiometry of the charges is 1:1. By contrast, dispersions of nanoparticles can be produced easily for nonstoichiometric complexes. An example is the complex of poly(ethylene imine) with dodecanoic acid. It forms a water-insoluble solid-state complex with a smectic A-like structure for a 1:1 stoichiometry.⁵ The same complex with an excess of poly(ethylene imine) of 50 mol % forms nanoparticles of the core–shell type that are useful as carriers for lipophilic drugs such as Q₁₀ and triiodothyronine.⁶ These particles exhibit hydrodynamic radii of 80–150 nm and high positive surface charges with zeta potentials of about +40 mV. Another way of producing nanoparticles is to use diblock copolymers with a complexing block and a noncomplexing block that stabilizes these particles. An example of this is shown in the complexes of dodecanoic acid with poly(ethylene oxide)-

block-poly(ethylene imine)s with linear, branched, and cyclic poly(ethylene imine) blocks.⁷ These complexes form core–shell particles with sizes around 200 nm, but their zeta potential is zero due to their electrostatic neutral shells of poly(ethylene oxide).

The aim of this work is also to prepare nanoparticles of complexes, but their diameters should be significantly smaller than the particles produced in our earlier studies (>50 nm). High specific interface areas between the particles and their surroundings should be generated in this way, and the zeta potentials of the particles should be adjustable. We prepared six different complexes for this purpose, whose molecular structures are shown in Figure 1. An alkylated (**H**) and a fluorinated fatty acid (**F**) of the same chain length (12 carbon atoms) will be compared in their complexation properties with the polyampholytes **P**₁, **P**₂, and **P**₃. It can be seen that the hydrophobicity of the rest, **R**, increases from **P**₁ to **P**₃.

Experimental Section

Materials. The maleamic acid, *N,N*-diallyl-*N,N*-dimethylammonium chloride, *n*-dodecanoic acid, perfluorododecanoic acid, sodium hydroxide, and toluene (HPLC grade) were supplied by Aldrich and used as received.

Monomer Synthesis. *N*-Phenylmaleamic Acid. A total of 98.06 g (1 mol) of maleic anhydride was dissolved in 500 mL of toluene and heated to 80 °C. Then 93.12 g (1 mol) of aniline, dissolved in 100 mL of toluene, was added in droplets and stirred at 80 °C for a further 2 h. The *N*-phenylmaleamic acid was observed as a precipitate after cooling the reaction mixture to room temperature. This product was separated, washed with 200 mL of toluene, and further purified by crystallization twice in ethanol (2 g of *N*-phenylmaleamic acid in 100 mL of ethanol). The yield was 138.6 g (72.5%). The composition was determined by 400 MHz ¹H NMR (Bruker DPX-400) in DMSO-*d*₆, δ (ppm): 6.3 (d, 1 H), 6.45 (d, 1 H), 7.1 (t, 1 H), 7.35 (t, 2 H), 7.65 (d, 2 H), 10.4 (s, 1 H), 13.15 (s, 1 H). The purity was checked by elemental

* Corresponding author. E-mail: andreas.thuenemann@iap.fhg.de.

(1) Zhou, S. Q.; Chu, B. *Adv. Mater.* **2000**, *12*, 545–556.

(2) Ober, C. K.; Wegner, G. *Adv. Mater.* **1997**, *9*, 17–31.

(3) MacKnight, W. J.; Ponomarenko, E. A.; Tirrell, D. A. *Acc. Chem. Res.* **1998**, *31*, 781–788.

(4) Goddard, E. D.; Ananthapadmanabhan, K. P. *Interactions of Surfactants with Polymers and Proteins*; CRC Press: Boca Raton, FL, 1993.

(5) Thünemann, A. F.; General, S. *Langmuir* **2000**, *16*, 9634–9638.

(6) Thünemann, A. F.; General, S. *J. Controlled Release* **2000**, *75*, 237–247.

(7) Thünemann, A. F.; General, S. *Macromolecules* **2001**, *34*, 6978–6984.

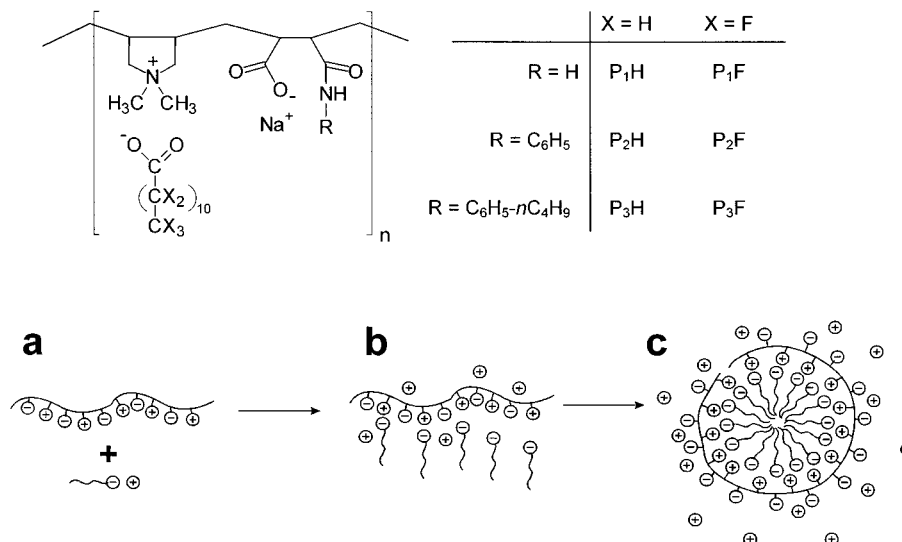


Figure 1. Complexes of the polyampholytes with dodecanoic acid (**P₁H**, **P₂H**, and **P₃H**) and perfluorododecanoic acid (**P₁F**, **P₂F**, and **P₃F**). The hydrophilicity of the polyelectrolytes decreases in the line **P₁**, **P₂**, **P₃**. The lower figure shows the formation of dressed micelles: (a) the polyampholyte and the sodium dodecanoate were mixed; (b) loose aggregates were formed by the complexation of polyampholyte and dodecanoate moieties (charge ratio, 1 positive to 1 negative); (c) reorganization of the complex to a compact polyampholyte dressed micelle.

analysis. Calculated (C₁₀H₉NO₃): C, 62.82; H, 4.75; N, 7.33. Found: C, 62.67; H, 4.76; N, 7.20.

***N*-(4-Butylphenyl)maleamic Acid.** The preparation of *N*-(4-butylphenyl)maleamic acid was analogous to that of *N*-phenylmaleamic acid. The product precipitates immediately after adding 4-butylphenylamine to a solution of maleic anhydride in the hot reaction mixture. The product was purified by recrystallizing it two times from ethanol (50 g/100 mL). The yield was 168.3 g (68.1%). The composition was determined by 400 MHz ¹H NMR (Bruker DPX-400) in DMSO-*d*₆, δ (ppm): 0.9 (t, 3H), 1.30 (sextet, 2H), 1.5 (quintet, 2H), 2.5 (t, 2H), 6.3 (d, 1H), 6.45 (d, 1H), 7.15 (d, 2H), 7.55 (d, 2H), 10.40 (s, 1H), 13.30 (s, 1H). The purity was checked by elemental analysis. Calculated (C₁₄H₁₉O₃): C, 67.99; H, 6.93; N, 5.66. Found: C, 67.99; H, 6.91; N, 5.69

Polymerizations. *Poly(N,N-diallyl-N,N-dimethylammonium-alt-maleamic Carboxylate).* The preparation of poly(*N,N*-diallyl-*N,N*-dimethylammonium-alt-maleamic carboxylate), **P₁** (cf. Figure 1), was similar to the procedure described earlier.⁸ A free radical polymerization was carried out in a 30.5% aqueous solution, which was adjusted to pH 8.5 using sodium hydroxide, at 60 °C for a period of 16 h. The reaction was carried out in a nitrogen atmosphere and with 2.0 g (0.0072 mol) of 4,4'-azobis(4-cyan-pentanoic carboxylate) (V501, Wako) as an initiator. **P₁** was purified by dialysis in water (membrane cutoff, 1000 g/mol) and subsequently freeze-dried. The yield was 46.0 g (47.9%). The analysis of **P₁** was as follows. ¹H NMR (D₂O, δ in ppm): 1.00–2.9 (8 H, –CH–, CH₂–), 3.0–3.5 (6 H, N–CH₃), 3.6–3.9 (4 H, N–CH₂–). Elemental analysis calculated (C₁₂H₂₀N₂O₃): C, 59.98; H, 8.39; N, 11.66. Found: C, 59.51; H, 8.83; N, 10.99. The sodium and chloride content was below 0.1%. The molecular weight of **P₁**, as determined by viscometry (in aqueous solution with a sodium chloride concentration of 1 mol L⁻¹, cf. method section), was *M_v* ≈ 20 000 g mol⁻¹, corresponding to a degree of polymerization of approximately 80.

Poly(N,N-diallyl-N,N-dimethylammonium-alt-N-phenylmaleamic Carboxylate). The synthesis and purification of poly(*N,N*-diallyl-*N,N*-dimethylammonium-alt-*N*-phenylmaleamic carboxylate), **P₂**, was the same as for **P₁**. The yield of **P₂** was 29.7 g (23.5%). ¹H NMR analysis (D₂O, δ in ppm): 0.6–3.9 (18 H, –CH–, CH₂–, CH₃), 6.9–7.6 (5 H, H_{arom}). Elemental analysis calculated (C₁₈H₂₄N₂O₃): C, 68.33; H, 7.66; N, 8.85. Found: C, 67.84; H, 7.86; N, 8.74. The sodium and chloride content was below 0.1%. The molecular weight of **P₂**, as determined by viscometry, was *M_v* ≈ 22 000 g mol⁻¹, corresponding to a degree of polymerization of approximately 70.

Poly(N,N-diallyl-N,N-dimethylammonium-alt-N-(4-butylphenyl)maleamic Carboxylate). The synthesis and purification of poly(*N,N*-diallyl-*N,N*-dimethylammonium-alt-*N*-(4-butylphenyl)maleamic carboxylate), **P₃**, was the same as for **P₁**. The yield of **P₃** was 33.1 g (22.2%). ¹H NMR analysis (D₂O, δ in ppm): 0.9–4.0 (27 H, –CH–, CH₂–, CH₃), 6.0–8.0 (4 H, H_{arom}). Elemental analysis calculated (C₂₂H₃₂N₂O₃): C, 70.94; H, 8.66; N, 7.52. Found: C, 69.69; H, 7.89; N, 7.38. The sodium and chloride content was below 0.1%. The molecular weight of **P₃**, as determined by viscometry, was *M_v* ≈ 22 000 g mol⁻¹, corresponding to a degree of polymerization of approximately 60.

Preparation of Complexes. A solution of 0.1 g of polyampholyte in 100 mL of water was adjusted to pH 8 using an aqueous solution of 0.1 mol L⁻¹ sodium hydroxide and heated to 90 °C. An aqueous solution (100 mL, 90 °C) of 1.0 equiv of the dodecanoic acid and perfluorododecanoic acid, respectively, was added in droplets to the polyampholyte solution, which was then adjusted to pH 8. The stoichiometries were calculated with respect to the charges such that the ratio of anionic surfactant headgroups (carboxylate) to cationic monomers (ammonium) was 1 to 1. The mixture was stirred for a further 60 min at 90 °C after the addition of the polyampholyte and then cooled to room temperature. All complexes were obtained as transparent aqueous solutions and remained stable for periods of more than 6 months.

Measurements. Viscosity measurements were performed using an Ubbelohde viscometer with automatic dilution (Viscoby 2, Lauda) at 25 °C. Water with sodium chloride at a concentration of 1 mol L⁻¹ was used as a solvent. The molecular weights of the polyampholytes were determined from the viscosity data by using the molecular weight dependency of the intrinsic viscosity, [η], according to the Mark–Houwink equation ([η] = *KM_v^a*), which is typically used for polyelectrolytes,⁹ where *M_v* is the viscosity-average molecular weight, and *a* and *K* are constants. We used *K* = 1.12 × 10⁻⁴ dL g⁻¹ and *a* = 0.82 for calibration, which are given for poly(*N,N*-diallyl-*N,N*-dimethylammonium chloride).¹⁰ These values are valid for a temperature of 25 °C and a sodium chloride concentration of 1 mol L⁻¹. The determination of the molecular weight using viscosity is a relative method resulting in apparent values for the polyampholytes. The sodium content was determined using an ICP Optima 3000 (Perkin-Elmer). Chloride was determined using potentiometric titration (TiNet

(8) Hahn, M.; Jaeger, W.; Schmolke, R.; Behnisch, J. *Acta Polym.* **1990**, *41*, 107–112.

(9) Dautzenberg, H.; Jaeger, W.; Kötz, J.; Philipp, B.; Seidel, Ch.; Stscherbina, D. *Polyelectrolytes: Formation, Characterization and Application*; Carl Hanser Verlag: Munich, 1994; p 218.

(10) Dautzenberg, H.; Jaeger, W.; Kötz, J.; Philipp, B.; Seidel, Ch.; Stscherbina, D. *Polyelectrolytes: Formation, Characterization and Application*; Carl Hanser Verlag: Munich, 1994; p 223.

2.4, Metrohm). The size of the nanoparticles was determined by dynamic light scattering, using a fixed angle (173°) ALV-NIBS/HPPS high-sensitivity submicron particle sizer. The samples were loaded into the measuring cell at a concentration (usually 1 g/L) that yields an optimum signal output (current count rate, 100 kHz). The number of replicants was five.

Analytical ultracentrifugation was carried out using a Beckman Optima XL-I ultracentrifuge (Beckman Counter, Palo Alto, CA) at (25 ± 0.2) °C and 50 000 rpm (acceleration 180 000*g*). Detection of the particles was carried out by applying UV-vis absorption detection at a wavelength of 210 nm (**P**₁) and 240 nm (**P**₂ and **P**₃), respectively. They were simultaneously detected using the Rayleigh interference optics. The measured radial concentration profiles were transformed into a sedimentation coefficient distribution by using eq 1 and then into an absolute particle size distribution using eq 2, that is,

$$s_i = \frac{\ln(r_i/r_m)}{\omega^2 t}, \quad (1)$$

$$d_i = \sqrt{\frac{18\eta s_i}{\rho_1 - \rho_2}} \quad (2)$$

where ω is the angular velocity, r is the radial distance from the center of rotation with the indices i = particle i and m = meniscus, d_i is the particle diameter of i , η is the solvent viscosity, s_i is the sedimentation coefficient of i , and ρ is the density with the indices 1 for water and 2 for the particle. The sedimentation coefficient distribution (eq 1) was calculated for a constant velocity of the particles where the centrifugal force acting on the particles was balanced by the frictional and buoyant forces. The validity of this assumption was checked by equal spacings between the individual scans. Equation 2 invokes Stokes' law implying that the particles must be spherical. If this is not the case, the diameter is that of an equivalent sphere. Furthermore, the particle size distributions calculated from eq 2 do not take diffusion into account which can be significant if the particles are very small such as those investigated in this work. Diffusion effects are suppressed, if a sufficiently high speed is selected so that the transport processes in the ultracentrifuge cell are clearly dominated by sedimentation. For the nanoparticles investigated in this work, this condition is sufficiently fulfilled by a rotation rate of 50 000 rpm. Nevertheless, diffusion effects cannot be suppressed completely, which leads to slightly broadened particle size distributions. Because of the very small particle size, the relative absorption of the individual particles corresponds directly to their mass fraction if the extinction coefficient does not change with the particle size. It was found that the evaluation of absorption and refractive index detection data results in the same particle size distribution, which justifies the assumption used in this study.

The density of the sedimented nanoparticles was determined with a vibrating tube densimeter, model DMA 60/602 (Anton Paar, Graz). The zeta potentials of the nanoparticles were determined with a Zetamaster (Malvern Instruments) averaging five measurements. We used the same solutions for dynamic light scattering and for zeta potential measurements.

The isothermal titration calorimetry (ITC) was carried out with a calorimeter type VP-ITC produced by MicroCal Inc. (Northampton, MA). The cell (volume, 1.44 mL) was filled with a fatty acid solution at different concentrations (2–4 mmol L⁻¹ for dodecanoic acid and 0.05–0.1 mmol L⁻¹ for perfluorododecanoic acid; the pH was 8). These values are significantly below the critical micelle concentrations (cmc's) of the fatty acids in their forms as carboxylates. We determined the cmc of sodium perfluorododecanoate to be 0.15 mmol L⁻¹. The reference cell contained water only. The injection syringe was filled with 288 μ L of a 1–20 mmol L⁻¹ polyampholyte solution, and a series of 10 μ L injections were made at a constant stirring rate of 380 rpm. With each injection, the fatty acid bound to the polyampholyte, leading to a characteristic heat signal. The baseline was subtracted to level the noninjection period signal to zero. The integration of the individual calorimeter traces measured the heat of binding which occurred at each injection step.

Results and Discussion

Mixing equimolar amounts of aqueous solutions of polyelectrolytes and ionic surfactants results in water-insoluble complexes of stoichiometric composition.¹¹ For clarity, molarities are given with respect to the positive (polyampholyte) and negative (dodecanoate) charges. The nanoprecipitation method,¹² which uses an excessive amount of polyelectrolytes^{6,13} or diblock copolymers,¹⁴ gives access to nanoparticles of complexes by which a macroscopic precipitation is avoided. The particle diameters, when using this technique, are typically in the range of 80–200 nm which makes the dispersions appear opaque. By contrast, the complexation of the polyampholytes **P**₁, **P**₂, and **P**₃ with dodecanoic acid, **H**, as well as with perfluorododecanoic acid, **F**, results in transparent solutions of the hydrogenated complexes **P**₁**H**, **P**₂**H**, and **P**₃**H** and the fluorinated complexes **P**₁**F**, **P**₂**F**, and **P**₃**F** (cf. Figure 1 for the chemical structures). The formation of larger aggregates and a macroscopic precipitation was not observed, a finding which was not expected. This was probably the result of the ampholytic character of the polymers. Because it was not clear whether discrete particles of complexes were formed or not, dynamic light scattering and ultracentrifugation measurements were carried out to determine this.

Nanoparticles. The dynamic light scattering measurements of the fluorinated complexes revealed that they formed discrete particles with diameters of 3.1 ± 0.3 nm (**P**₁**F**), 3.2 ± 0.3 nm (**P**₂**F**), and 2.7 ± 0.5 nm (**P**₃**F**). The hydrogenated complexes formed particles with sizes of the same order of magnitude as the fluorinated particles, but their mean diameters spread over a broad range (2–4 nm, **P**₁**H**; ≈ 3 nm, **P**₂**H**; ≈ 3 nm, **P**₃**H**). In contrast to their complexes, the dynamic light scattering data of the neat polyampholytes indicated only scattering objects with hydrodynamic radii smaller than 1.5 nm. Therefore, the presence of aggregates of the polyampholytes due to intermolecular salt formation can be ruled out. This is remarkable because many polybetaines, that is, polymers with a positive and negative charge at the same monomer unit, typically have a strong tendency to form intermolecular aggregates.^{15–17} It is possibly due to the alternating structure of cationic and anionic monomeric units along the polymeric chains of **P**₁, **P**₂, and **P**₃ that they do not display self-aggregation.

One of the most reliable experimental methods for the determination of particle size distributions is analytical ultracentrifugation, which allows an accuracy in the particle size distribution determination down to angstrom resolution.¹⁸ Therefore, we performed sedimentation velocity experiments of the complexes at different concentrations (1×10^{-3} to 2 g L⁻¹). It was found that the particles sediment well at a rotation rate of 5×10^4 rpm. We measured the density of the particles (cf. Table 1) and calculated their size distributions as described in the Experimental Section; the results are shown in Figures

(11) Goddard, E. D.; Ananthapadmanabhan, K. P. *Interactions of Surfactants with Polymers and Proteins*; CRC Press: Boca Raton, FL, 1993.

(12) Duchene, D.; Ponchel, G.; Wouessidjewe, D. *Adv. Drug Delivery Rev.* **1999**, *36*, 29–40.

(13) Thünemann, A. F.; General, S. *Int. J. Pharm.* **2001**, *230*, 11–24.

(14) Thünemann, A. F.; Beyermann, J.; Kukulka, H. *Macromolecules* **2000**, *33*, 5906–5911.

(15) Ali, S. A.; Rasheed, A. *Polymer* **1999**, *40*, 6849–6857.

(16) Niu, A. Z.; Liaw, D. J.; Sang, H. C.; Wu, C. *Macromolecules* **2000**, *33*, 3492–3494.

(17) Bohrisch, J.; Grosche, O.; Wendler, U.; Jaeger, W.; Engelhardt, H. *Macromol. Chem. Phys.* **2000**, *201*, 447–452.

(18) Cölfen, H.; Pauck, T. *Colloid Polym. Sci.* **1997**, *275*, 175–180.

Table 1. Characteristics of the Nanoparticles Formed by the Polyampholyte Complexes as Determined by the Analytical Ultracentrifugation, Dynamic Light Scattering, and Zeta Potential Measurements^a

| complex | density (g/cm ³) | degree of sedimentation [%] | diameter from UZ [nm] | diameter from DLS [nm] | zeta potential [mV] |
|-----------------------|------------------------------|-----------------------------|------------------------|------------------------|---------------------|
| Hydrogenated | | | | | |
| P₁H | 1.256 | 40 | 2.7 ± 0.1 ^b | 2–4 | +25 ± 10 |
| P₂H | 1.273 | 80 | 3.9 ± 0.1 ^b | ≈3 | -20 ± 4 |
| P₃H | 1.103 | 100 | 6.0 ± 0.1 | ≈3 | -31 ± 5 |
| Fluorinated | | | | | |
| P₁F | 1.654 | 75 | 5.1 ± 0.1 | 3.1 ± 0.6 | -47 ± 5 |
| P₂F | 1.754 | 90 | 3.9 ± 0.1 | 3.2 ± 0.9 | -48 ± 5 |
| P₃F | 1.442 | 100 | 4.0 ± 0.1 | 2.7 ± 0.8 | -56 ± 5 |

^a The concentrations of the nanoparticles were 2% (w/w) in aqueous solutions. ^b The maximum was determined as the shoulder in the plot of the relative particle concentration in Figure 2.

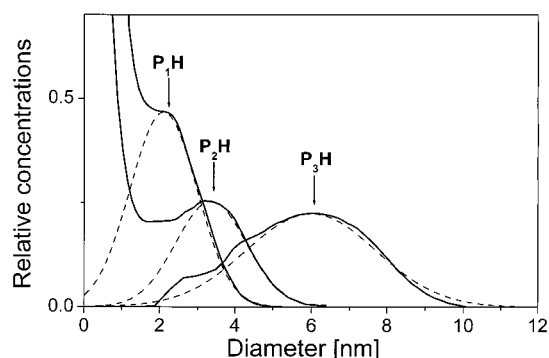


Figure 2. Particle size distributions of the polyampholyte complexes with dodecanoic acid, **P₁H**, **P₂H**, and **P₃H**, as determined by the analytical ultracentrifugation measurements. The concentrations were 1 g L⁻¹.

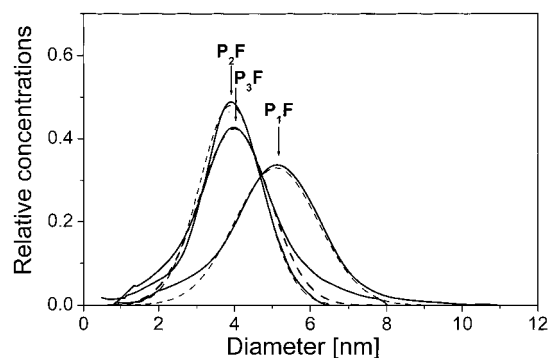


Figure 3. Particle size distributions of the polyampholyte complexes with perfluorododecanoic acid, **P₁F**, **P₂F**, and **P₃F**, as determined by the analytical ultracentrifugation measurements. The concentrations were 1 g L⁻¹.

2 and 3. It can be seen in Figure 3 that the particles of the fluorinated complexes are almost of the same size and, further, that their size distributions are narrow. Gaussian fits were found to be suitable for their quantification resulting in mean diameters of 5.1 ± 0.1 nm (**P₁F**), 3.9 ± 0.1 nm (**P₂F**), and 4.0 ± 0.1 nm (**P₃F**) (cf. dashed lines in Figure 3). The widths of the size distributions as described by the standard deviations were 1.1 nm (20% of the mean size, **P₁F**), 0.8 nm (20%, **P₂F**), and 0.9 nm (23%, **P₃F**). In contrast to the fluorinated complexes, the sizes of the hydrogenated complex particles were not that uniform. Their mean diameters were 2.7 ± 0.1 nm (**P₁H**), 3.9 ± 0.1 nm (**P₂H**), and 6.0 ± 0.1 nm (**P₃H**). The widths of their distributions were 0.6 nm (22%, **P₁H**), 0.9 nm (23%, **P₂H**), and 1.7 nm (28%, **P₃H**). The strong increase in the relative concentrations at diameters smaller than 1 nm for **P₁H** and **P₂H** was probably due to noncomplexed polyampholyte chains and does not need to be taken into account for fitting. Control experiments

of the neat polyampholytes revealed that no sedimenting objects of sizes significantly larger than 1 nm were present. This supported the results from dynamic light scattering, which ruled out the aggregation of the neat polyampholytes. In summary, the diameters as determined by the analytical ultracentrifugation agreed well with the values determined by dynamic light scattering (cf. Table 1).

We conclude that the particle sizes of the fluorinated complexes are, as a first approximation, independent of the modification of the polyampholyte. However, the particle sizes of the hydrogenated complexes became larger when the hydrophobicity of the polyampholyte increases (**P₁** < **P₂** < **P₃**). The most simple geometric model is that the particles consist of compact cores, which are formed by the hydrophobic surfactant chains, and a hydrophilic shell like a typical surfactant micelle.¹⁹ But the difference between the surfactant micelle and the particles of the complexes is that the low molecular weight counterions are replaced by the polyampholytes. This means that large molecules with approximately 60–80 binding sites stick on the micelle surface instead of moving like highly mobile single-charged ions. We assumed that this stabilized the particles. The polyampholytes are wrapped around the micelle which can be figuratively described as a dressed micelle.

The stability of the particles results from the interplay of ionic and hydrophobic interactions. Because they are not chemically cross-linked, it must be assumed that the particles dissolve at small concentrations. Therefore, the particles were successively diluted using stock solutions. After 2 days of storage at room temperature, we investigated them using ultracentrifugation. Experiments were carried out at pH 8 with particle concentrations in the range of 1 × 10⁻³ to 2 g L⁻¹. Examples of **P₂F** are shown in Figure 4. It can be seen there that the size distributions of the particles are constant within this large range of concentrations. Neither aggregation at the higher concentrations nor dissolution at the lower concentrations was observed within a test period of 6 months. The experiments were repeated for the other complexes, and the results are summarized in Figure 5. It can be seen there that no particles were detected for concentrations of lower than 1 g L⁻¹ (**P₁F** and **P₁H**), 10⁻² g L⁻¹ (**P₂F** and **P₂H**), and 2 × 10⁻² g L⁻¹ (**P₃F** and **P₃H**). These concentration values seem to be reasonable for the critical aggregation concentrations (cac's) of the complexes. Obviously the cac depends significantly on the type of polyampholyte. The complexes with the hydrophilic rest H have a higher cac than the complexes with hydrophobic rests phenyl and 4-butylphenyl. This was our expectation because it is well-known from the literature on polyelec-

(19) Israelachvili, J. N. In *Physics of Amphiphiles: Micelles, Vesicles and Microemulsions*; Elsevier: New York, 1985; p 42.

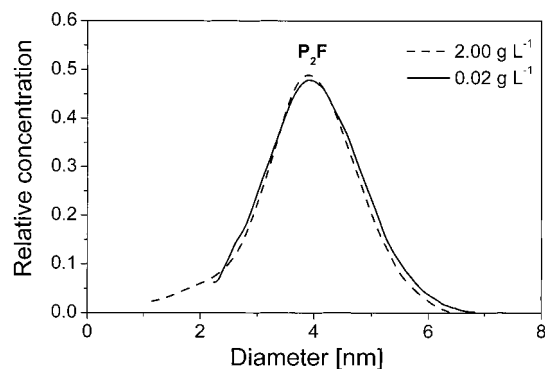


Figure 4. Particle size distributions of the fluorinated complex P_2F at concentrations of 0.02 and 2 $g L^{-1}$ as determined by the analytical ultracentrifugation measurements.

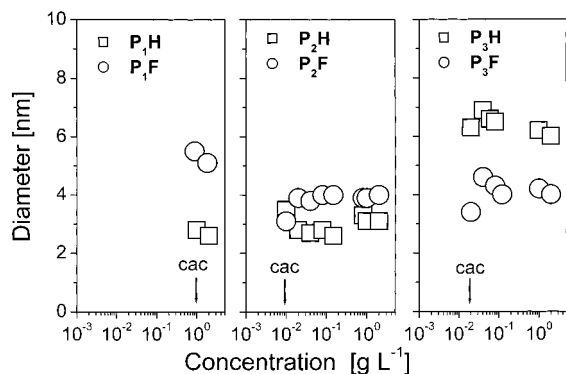


Figure 5. Mean diameters of the fluorinated and hydrogenated nanoparticles as a function of their concentrations. The critical aggregation concentrations (indicated by arrows) are 1 $g L^{-1}$ (P_1F and P_1H), 10^{-2} $g L^{-1}$ (P_2F and P_2H), and 2×10^{-2} $g L^{-1}$ (P_3F and P_3H).

trolyte-surfactant complexes that the cac's depend significantly on the nature of the polyelectrolyte.^{20,21}

On the other hand, it is surprising that we found no significant difference in the cac's of the fluorinated and the hydrogenated complexes of the same polyampholytes. The cmc's of the sodium salts of dodecanoic acid (31.2 $mmol L^{-1}$)²² and perfluorododecanoic acid (0.15 $mmol L^{-1}$)²³ differ by a factor of 200. By contrast, the cac's of their complexes with the polyampholytes do not differ significantly. This is surprising because perfluorododecanoic acid is more hydrophobic than dodecanoic acid, from which it could be expected that this can also lower the cac of the particular complex. But here, it seems that the hydrophobic modification of the polyelectrolyte has the major influence on the cac of the complexes.

The degree of complexation can be approximated by the amount of sedimenting polyelectrolytes as detected by the ultracentrifugation measurements. It was found that the percentage of sediment increases in the line 40% (P_1H), 80% (P_2H), and 100% (P_3H) for the hydrogenated particles and in the line 75% (P_1F), 90% (P_2F), and 100% (P_3F) for the fluorinated particles (see Table 1). We interpret this also as a result of the increasing hydrophobicity of the rest R from P_1 to P_3 .

We assume that the long-term stability of the nanoparticles results from their charge stabilization. Therefore,

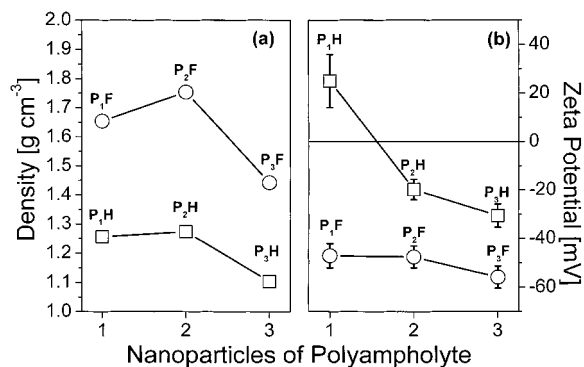


Figure 6. (a) The density of the nanoparticles of the complexes with dodecanoic acid (squares) and perfluorododecanoic acid (circles). (b) Zeta potentials of the nanoparticles with dodecanoic acid (squares) and perfluorododecanoic acid (circles).

Table 2. Stability of the Nanoparticles in Solution at Different pH Values and a Concentration of 1% (w/w)^a

| Complex | pH Value | 2 | 3 | 4 | 5 | 6 | 7 | 8 | 9 | 10 | 11 | 12 | 13 |
|---------|----------|---|---|---|---|---|---|---|---|----|----|----|----|
| P_1H | | | | | | | | | | | | | |
| P_2H | | | | | | | | | | | | | |
| P_3H | | | | | | | | | | | | | |
| P_1F | | | | | | | | | | | | | |
| P_2F | | | | | | | | | | | | | |
| P_3F | | | | | | | | | | | | | |

^a The gray areas indicate the pH values where the particles are stable, and the white areas indicate where the particles precipitate. The temperature was 25 °C.

we measured their zeta potentials, which are shown in Figure 6b and Table 2. It can be seen there that the zeta potentials of the fluorinated complexes are highly negative with values in the range of -47 mV (P_1F) to -56 mV (P_3F). The differences in the zeta potentials of the hydrogenated complexes are more pronounced. They decrease in a line from $+25$ mV (P_1H) to -20 mV (P_2H) to -31 mV (P_3H); that is, their zeta potentials decrease strongly with the increasing hydrophobicity of the rest R. We interpreted the zeta potentials of the nanoparticles with reference to the dressed micelle model,^{24,25} which addressed the question as to why counterions should bind to micelles. The dressed micelle model explains theoretically the fact that micelles are less than fully ionized at all concentrations. The degree of ionization is typically in the range of 20–50%. Applying this to the complexes, we supposed that the aggregation of the complexes took place through a polyampholyte-induced micellization process beyond the cac.

We propose that the particle formation starts with the binding of dodecanoate moieties to the polyampholytes, which then form loose aggregates. These aggregates reorganize into compact particles with a core of alkyl chains after the saturation of the polyampholytes with the carboxylates. Finally the polyampholyte chains are bound to the surface of dodecanoate micelles because of ion-ion associations. A scheme of the structure formation is shown in Figure 1. It is probable that the number of cationic counterions (protons and sodium ions) that are condensed on the particle surface decreases with the increasing hydrophobicity of the rest R. This would explain the decrease of the zeta potential in the same line. Further, perfluorododecanoic acid is a stronger acid than dodecanoic acid which explains why the fluorinated complexes display lower zeta potentials than the hydrogenated ones.

(20) Goddard, E. D. *Colloids Surf.* **1986**, *19*, 301–329.

(21) Hayakawa, K.; Kwak, J. C. T. *J. Phys. Chem.* **1982**, *86*, 3866–3870.

(22) Ingram, T.; Jones, M. N. *Trans. Faraday Soc.* **1969**, *65*, 297.

(23) Sander, K. Ph.D. Thesis, Technical University Berlin, Germany, 2002; p 96.

(24) Evans, D. F.; Mitchell, D. J.; Ninham, B. W. *J. Phys. Chem.* **1984**, *88*, 6344.

(25) Hayter, J. B. *Langmuir* **1992**, *8*, 2873–2876.

The length of perfluorododecanoic acid with a fully extended chain is 1.7 nm as calculated by the same method as used for the perfluorinated acids.²⁶ Such an all-trans conformation seems to be reasonable for perfluorododecanoate because of the stiffness of the fluorocarbon chain. Twice the length of the perfluorododecanoic acid in its extended form (3.4 nm) is the maximum diameter of a spherical micelle without its surroundings of polyampholytes. When allowing for a shell of polyampholyte chains, we estimated diameters in the range of 4–5 nm for spherical particles, which matched well with the particle sizes found for the fluorinated particles. The smaller diameters of the particles of **P₁H** and **P₂H** are indicative of more coiled conformations of the alkyl chains. This is reasonable because it would result in less extended alkyl chains than for the fluorinated chains. Diameters greater than 4–5 nm are possible if the particle shape is, for example, oblate or disklike. This could be an explanation for the comparatively large diameters of the **P₃H** particles.

Our next question was, how stable are the particles when the pH value is changed from pH 8 to more acidic or basic values? To answer this question, the solutions of the nanoparticles with concentrations of 2 g L⁻¹ were altered to within a range of pH 2–13 by adding hydrochloric acid or sodium hydroxide, respectively. The results are summarized in Table 2. It can be seen there, as indicated by bars, that neither turbidity nor precipitation was observed for all the complex dispersions in the range of pH 6 to pH 13. The latter was the highest pH value used in our investigations. Further, the particle sizes were also constant within this range. The situation is different at low pH values, where all complexes precipitate, but the set-on points were different. Precipitation started at pH < 6.0 (**P₂H**, **P₃H**, and **P₃F**), pH < 5.5 (**P₁H**), pH < 5.0 (**P₂F**), and pH < 4.0 (**P₁F**). We interpreted the occurrence of precipitation at low pH values as being predominately the result of the protonation of the carboxylic acid groups of the polyampholytes. This destabilizes the particles by lowering the particle charges, which is followed by aggregation and precipitation. The fluorinated particles precipitate significantly more slowly and at lower pH values than the hydrogenated particles. The reason for this was presumably the lower zeta potential of the fluorinated particles compared to the hydrogenated particles. The reason for the positive value of the zeta potential of **P₁H** was not clear.

When considering the densities of the complex particles, we observed two trends (cf. Figure 6a). First, the densities of the fluorinated complexes were drastically higher (1.444–1.754 g cm⁻³) than those of the hydrogenated complexes (1.103–1.273 g cm⁻³). Second, the densities of the complexes where the polyampholyte residues were R = H and R = phenyl are similar but the complexes with R = butylphenyl are significantly lower than these (cf. Figure 4a and Table 1). The higher density of the fluorinated complex particles compared to that of the hydrogenated particles is simply a result of the high density of the perfluoroalkyl chains that has an upper limit of about 2 g cm⁻³, which is that of amorphous poly(tetrafluoroethylene).²⁷ Both complexes of polyampholyte **P₃** showed a lower density than the corresponding complexes of **P₁** and **P₂**. This is probably due to the less dense packing of the **P₃** complexes in their particles.

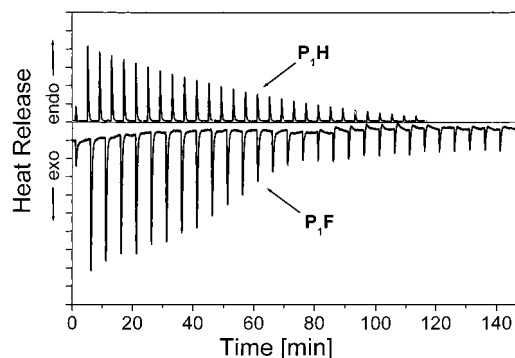


Figure 7. Heat release of the complexation of **P₁H** and **P₁F** as a function of time for the determination of their cumulative heat release of complex formation. The surfactants **H** and **F** were submitted to the sample chamber, and the polyampholyte **P₁** was added in a sequence of injections. It can be seen that the heat flow per injection is exothermic for **P₁F** and endothermic for **P₁H**.

Table 3. Cumulative Heat Releases Measured for the Complex Formation at a Polyampholyte/Surfactant Ratio of 1 (H, See Figure 8) and for the Dilution of the Polyampholytes (*H_{dil}*)^a

| | <i>H</i> | <i>H</i> | <i>H_{dil}</i> |
|-----------------------|-------------------------|-----------------------|-------------------------|
| complex | [kJ mol ⁻¹] | complex | [kJ mol ⁻¹] |
| P₁H | +25 | P₁F | -71 |
| P₂H | +20 | P₂F | -26 |
| P₃H | -11 | P₃F | -53 |
| | | P₁ | -0.3 |
| | | P₂ | -0.1 |
| | | P₃ | -0.2 |

^a Isothermal titration calorimetry was used for these measurements.

We were interested in the binding powers of the dodecanoates with the polyampholytes. This was observed by isothermal microcalorimetry as shown in Figure 7. The dodecanoates were dissolved in water below their cmc's at 25 °C. Then the polyampholytes were injected to the dodecanoate solutions and the heat flow was measured. It can be seen in Figure 7 that each injection was accompanied by an endothermic response when **P₁** is added to **H** and that the response was exothermic when **P₁** was added to **F**. The intensity of the response decreased successively with the increasing number of injections. Thus, it is obvious that the formation of the **P₁H** complex is endothermic while that of **P₁F** is exothermic. The same experiment was carried out for the two other polyampholytes. Then the heat releases of complexation were determined by the integration of the heat flow signals. Before this was done, the dilution heat releases of the pure polyampholytes were determined and proved to be very small (-0.1 to -0.3 kJ mol⁻¹, cf. Table 3). This confirmed our conclusion drawn from the light scattering and ultracentrifugation measurements, namely, that the polyampholytes themselves do not form intermolecular aggregates.

The cumulative heat releases due to the complex formation are shown in Figure 8 as a function of the polyampholyte-to-surfactant ratio. It can be seen there that the cumulative heat release for the complex formation is strongly negative for all fluorinated complexes. At a 1:1 stoichiometry (which was used prior to the particle formation), we determined values of -71 kJ mol⁻¹ (**P₁F**), -26 kJ mol⁻¹ (**P₂F**), and -53 kJ mol⁻¹ (**P₃F**). For clarity, mole refers to the polyampholyte monomeric units (a cationic plus an anionic). The cumulative heat releases for the hydrogenated complexes at a 1:1 stoichiometry were determined to be 25 kJ mol⁻¹ (**P₁H**), 20 kJ mol⁻¹ (**P₂H**), and -11 kJ mol⁻¹ (**P₃H**). It can be seen from the curves that the cumulative heat release values did not,

(26) Burkitt, S. J.; Ottewill, R. H.; Hayter, J. B.; Ingram, B. T. *Colloid Polym. Sci.* **1987**, *265*, 619.

(27) van Krevlen, D. W. *Properties of Polymer*; Elsevier: Amsterdam, 1990.

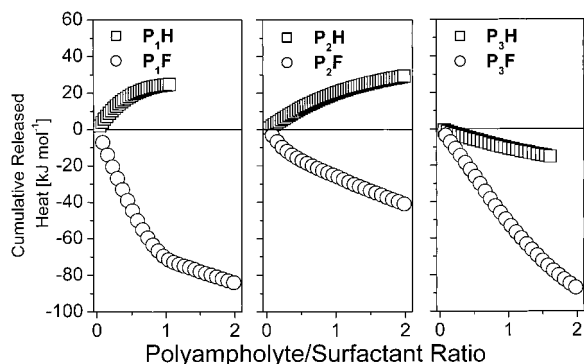


Figure 8. Cumulative heat releases for the complex formations of P_1H and P_1F (left-hand figure), P_2H and P_2F (middle figure), and P_3H and P_3F (right-hand figure) as a function of the polyampholyte-to-surfactant ratio. The ratios were calculated with respect to the cationic and anionic charges, respectively.

despite P_1H , reach a constant value. This means that further enthalpic interactions between the polyampholyte and the surfactants took place at higher polyampholyte-surfactant ratios than 1:1. The development of models of the binding between the polyampholytes and the surfactants on the basis of isothermal calorimetry measurements seems to be possible but is beyond the scope of the current work. Detailed studies have been carried out by Holzwarth et al. for the binding of sodium dodecyl sulfate to poly-(ethylene imine).²⁸ There is probably a correlation between the ability to form defined particles and the heat release of complex formation. The complexes P_1F , P_2F ,

and P_3F which display particles with a narrow particle size distribution have a highly negative complex formation cumulative heat release value. P_3H , the one with the broadest particle size distribution, displays a small negative value, while P_1H and P_2H , which both have a significant amount of noncomplexed polyampholyte, display a slightly positive cumulative heat release.

Conclusion

We have shown that the 1:1 complexation of polyampholytes with fluorinated and hydrogenated surfactants of the same chain length results in the formation of long-term stable nanoparticles in the form of dressed micelles. The particle sizes are constant over a large range of concentrations. The cac's of the complex particles depend on the hydrophilic/hydrophobic modification of the polyampholyte but not on whether the surfactant has a hydrogenated or fluorinated alkyl chain. Zeta potential measurements reveal that the particles are stabilized ionically. The particles are not sensitive to a basic pH value, but they aggregate at pH values lower than about 4–6. The complex formation is strongly exothermic for the fluorinated surfactant and endothermic to slightly exothermic for the hydrogenated surfactant.

Acknowledgment. We thank Dr. Görnitz for the analytical ultracentrifugation measurements and Dr. Hahn for his general support. The financial support of the Deutsche Forschungsgemeinschaft (DFG-Schwerpunkt "Polyelektrolyte mit definierter Molekülarchitektur", Grants Lo418/7-1 and JA 555/6-1) and the support of the Max Planck Society and the Fraunhofer Society are gratefully acknowledged.

(28) Li, Y.; Ghoreishi, S. M.; Warr, J.; Bloor, D. M.; Holzwarth, J. F.; Wyn-Jones, E. *Langmuir* **2000**, *16*, 3093–3100.